Supplementary Figures

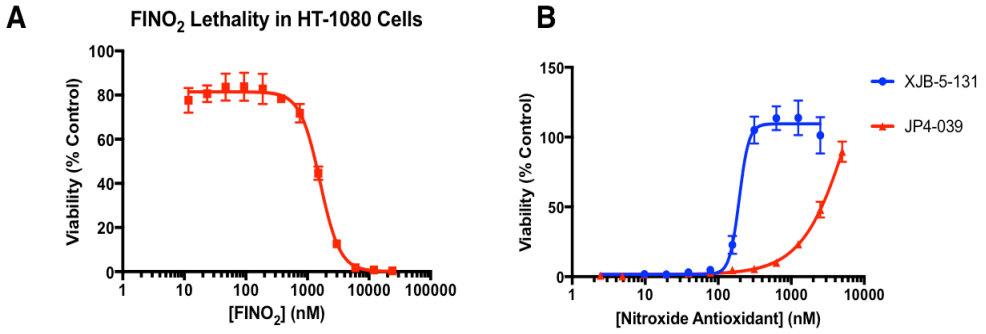

Supplementary Figure 1. (A) Dose-dependent lethality of $FINO_2$ in HT-1080 cells. Experiments were performed in biological triplicate. (B) Dose-dependent rescue of ferroptosis-suppressing nitroxides on HT-1080 cells treated with $FINO_2$ (10 μM). Viability for (A) and (B) was measured 24 h after compound addition using presto blue. Experiments were performed in biological triplicate. Data are plotted as the mean ± s.d..

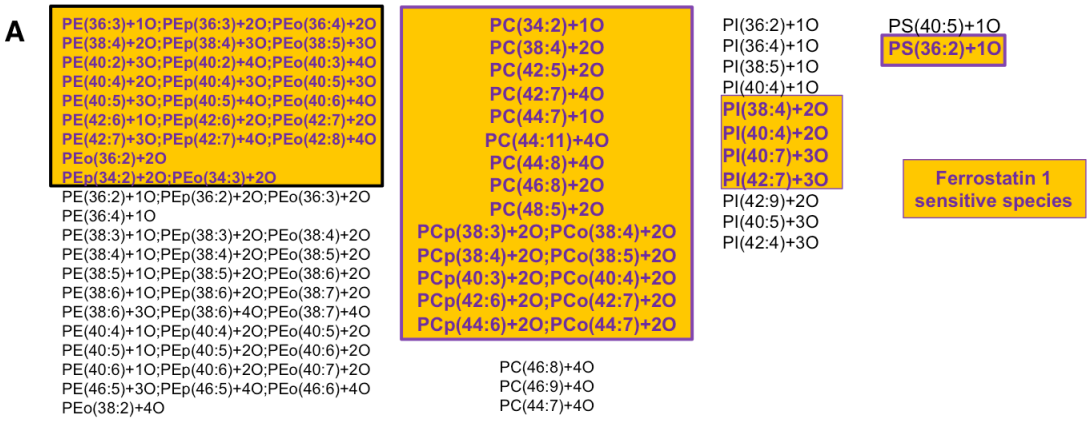

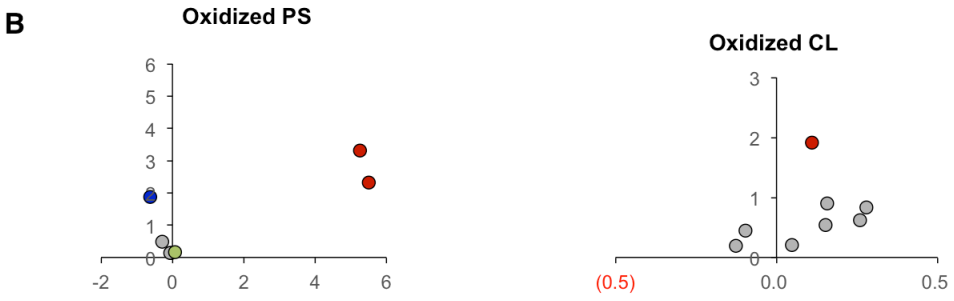

Supplementary Figure 2. (A) Lipids oxidized in HT-1080 cells treated with $FINO_2$ (10 μM). Lipids that were not upregulated when co-treated with ferroptosis suppressor ferrostatin (2 μM) are boxed in orange. PE: Phosphatidylethanolamine, PC: Phosphatidylcholine, PI: Phosphotidylinositol, PS: Phosphatidylserine. (B) Change in oxidized phosphatidylserine (PS) and cardiolipin (CL) following $FINO_2$ treatment in HT-1080 cells (10 μM). Green and gray circles indicate no change, red circles indicate an increase in abundance and blue circles indicate depletion.

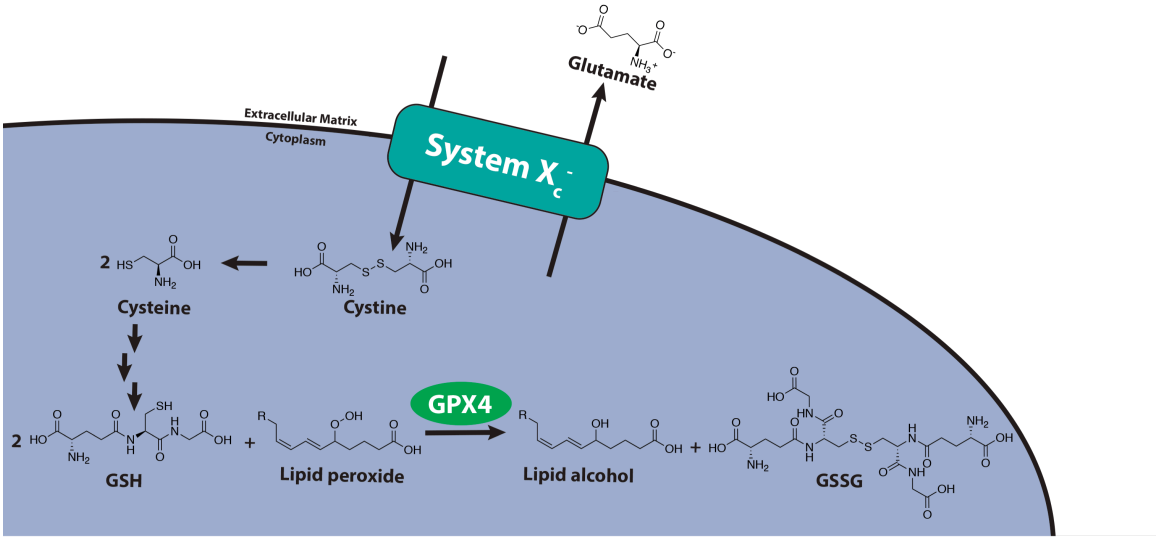

Supplementary Figure 3. Cystine import via system x_c^- provides cysteine required for synthesis of glutathione (GSH), a necessary cofactor for the lipid peroxide-reducing enzyme GPX4.

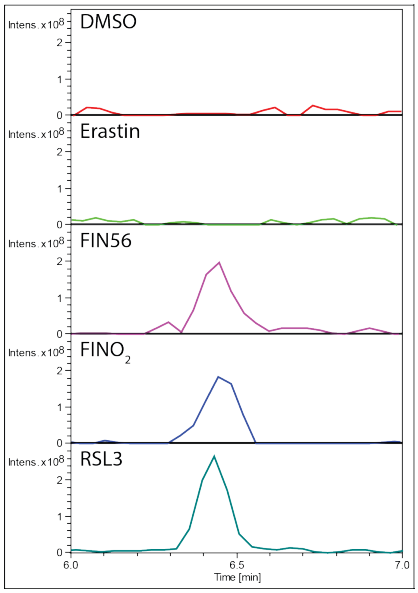

Supplementary Figure 4. Effect of ferroptosis inducers on the *in vitro* activity of GPX4 from treated HT-1080 cells. Cells were treated with DMSO, erastin (10 μM), FIN56 (5 μM), or $FINO_2$ (10 μM) for 6 h or RLS3 (0.5 μM) for 2 h. Cells were lysed and lysates were treated with PCOOH and GSH; after incubation (45 min) mixtures were extracted for lipids and the abundance of PCOOH was measured by LC-MS. Three independent experiments were performed with similar results.

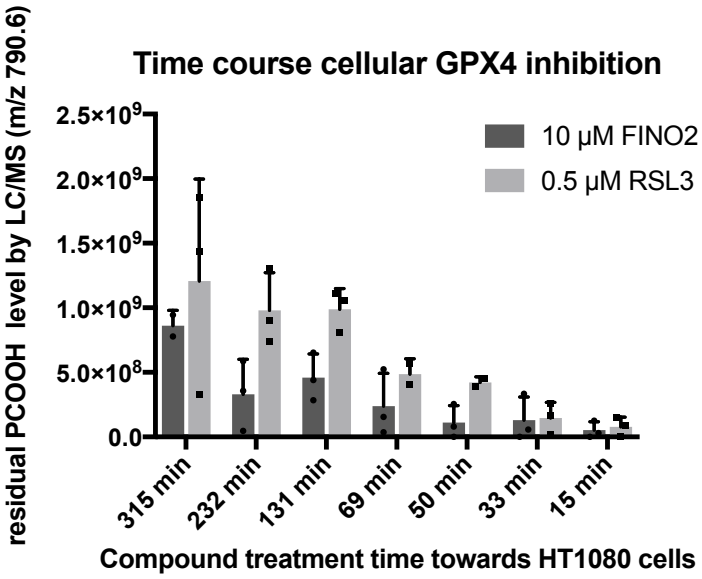

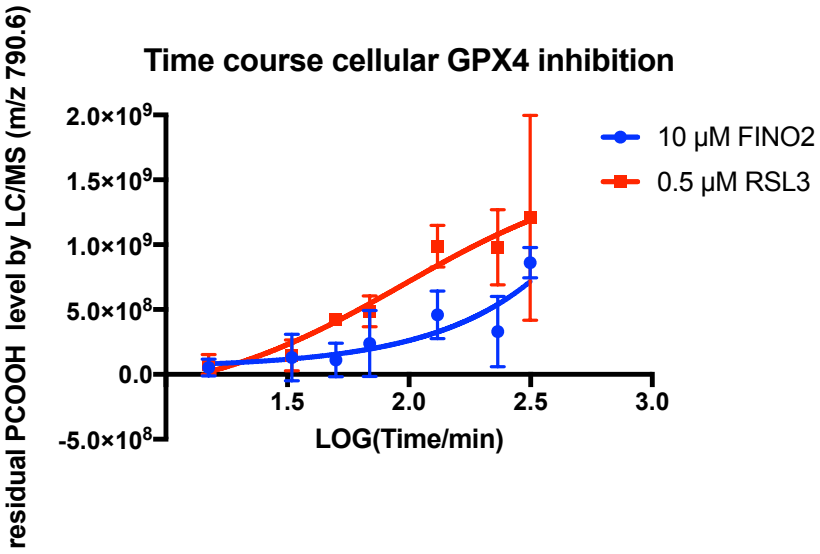

Supplementary Figure 5. Time dependent inhibition of GPX4-mediated PCOOH reduction by RSL3 and $FINO_2$. Data are plotted as the mean ± s.d.. Experiments were performed in triplicate with biologically independent samples.

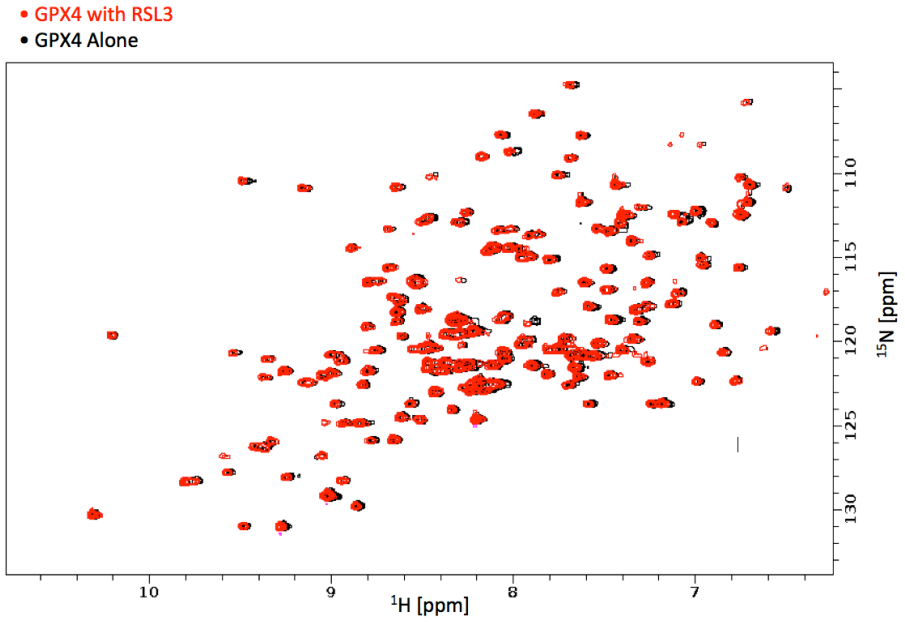

Supplementary Figure 6. HSQC NMR of GPX4^{U46C} (10 μM) with RSL3 (100 μM).

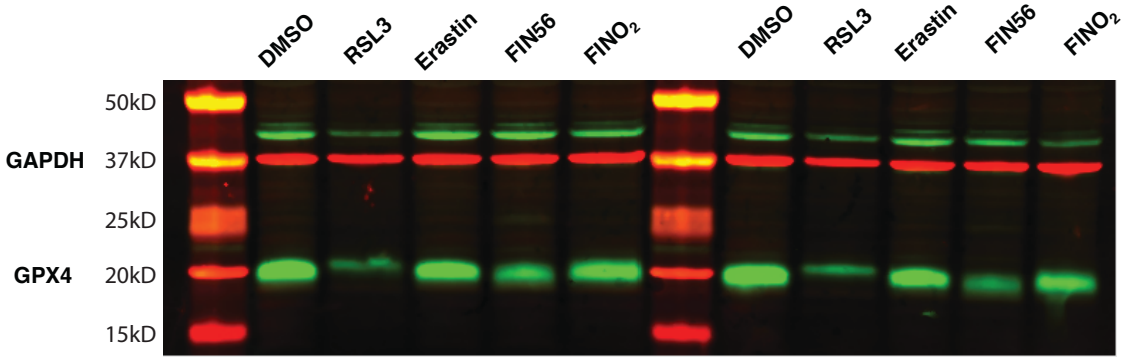

Supplementary Figure 7. Representative blot image from figure 3E.

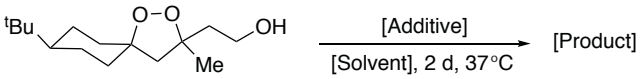

$FINO_2$ (**4**)

Entry	[Additive][a]	[Solvent]	[Product]
1	cysteine	DMSO-d_6	no reaction
2	GSH	DMSO-d_6	no reaction
3	arachadonic acid	CD_3CN	no reaction
4	selenocysteine	DMSO-d_6	no reaction
5	ebselen	DMSO-d_6	no reaction
6	Et_3N	DMSO-d_6	no reaction
7	KOH	DMSO-d_6	no reaction
8	DCl, KCl, NaCl	D_2O/DMSO-d_6	no reaction

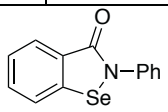

ebselen (**43**)

Supplementary Figure 8. Stability of $FINO_2$ under various reactive conditions.

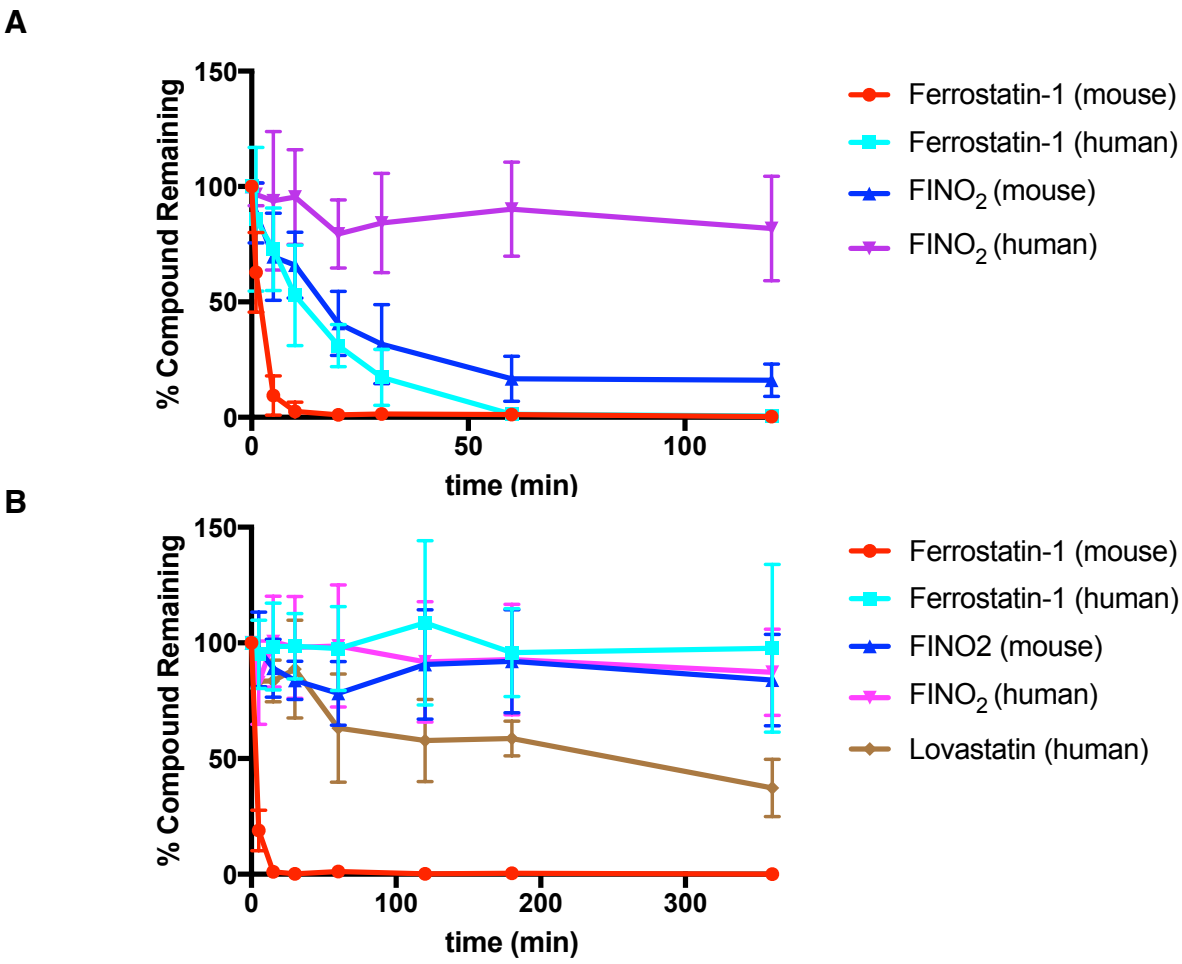

Supplementary Figure 9. Metabolic stability of $FINO_2$. (A) Stability of $FINO_2$ in mouse and human liver microsomes. (B) Stability of $FINO_2$ in mouse and human plasma. Experiments were performed in biological triplicate. Data are plotted as the mean ± s.d..

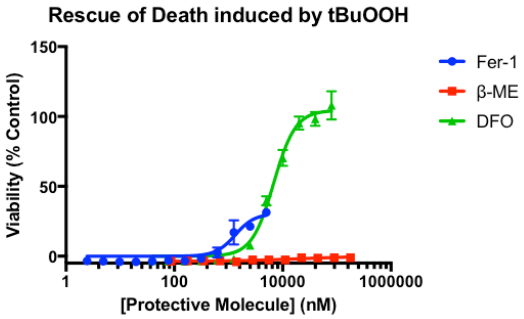

Supplementary Figure 10. Dose-dependent effect of ferroptosis-suppressing compounds on lethality initiated by *t*BuOOH (150 µM). Viability was measured 24 h after compound addition using presto blue. Experiments were performed in biological triplicate. Data are plotted as the mean ± s.d..

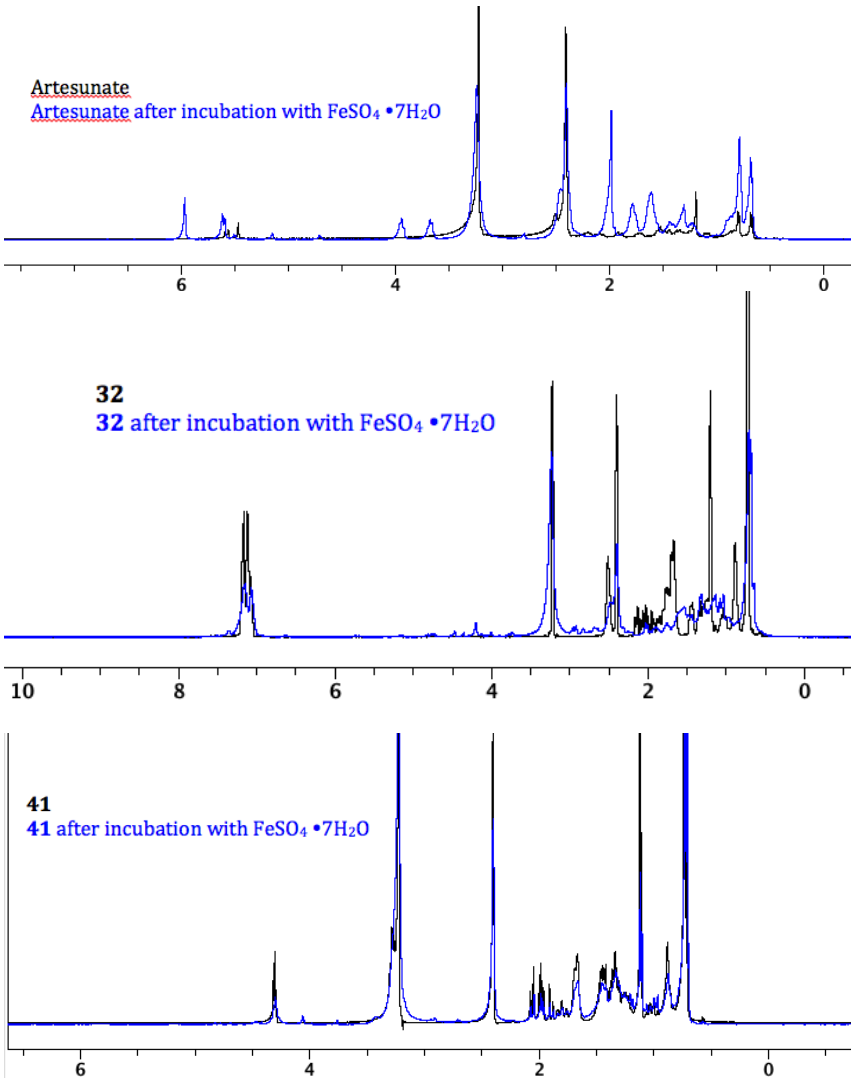

Supplementary Figure 11. Stability of Artesunate and $FINO_2$ analogues in the presence of $FeSO_4$

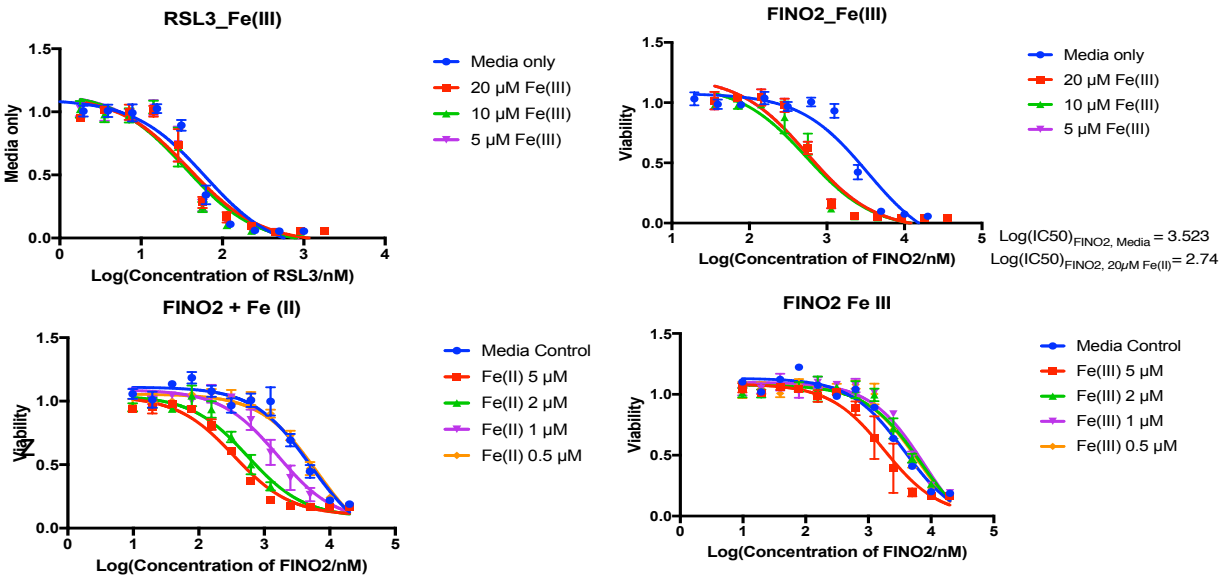

Supplementary Figure 12. Potency changes ferroptosis induction by $FINO_2$ and RSL3 in the presence of iron salts. Experiments were done in biological triplicate. Data are plotted as the mean ± s.d..

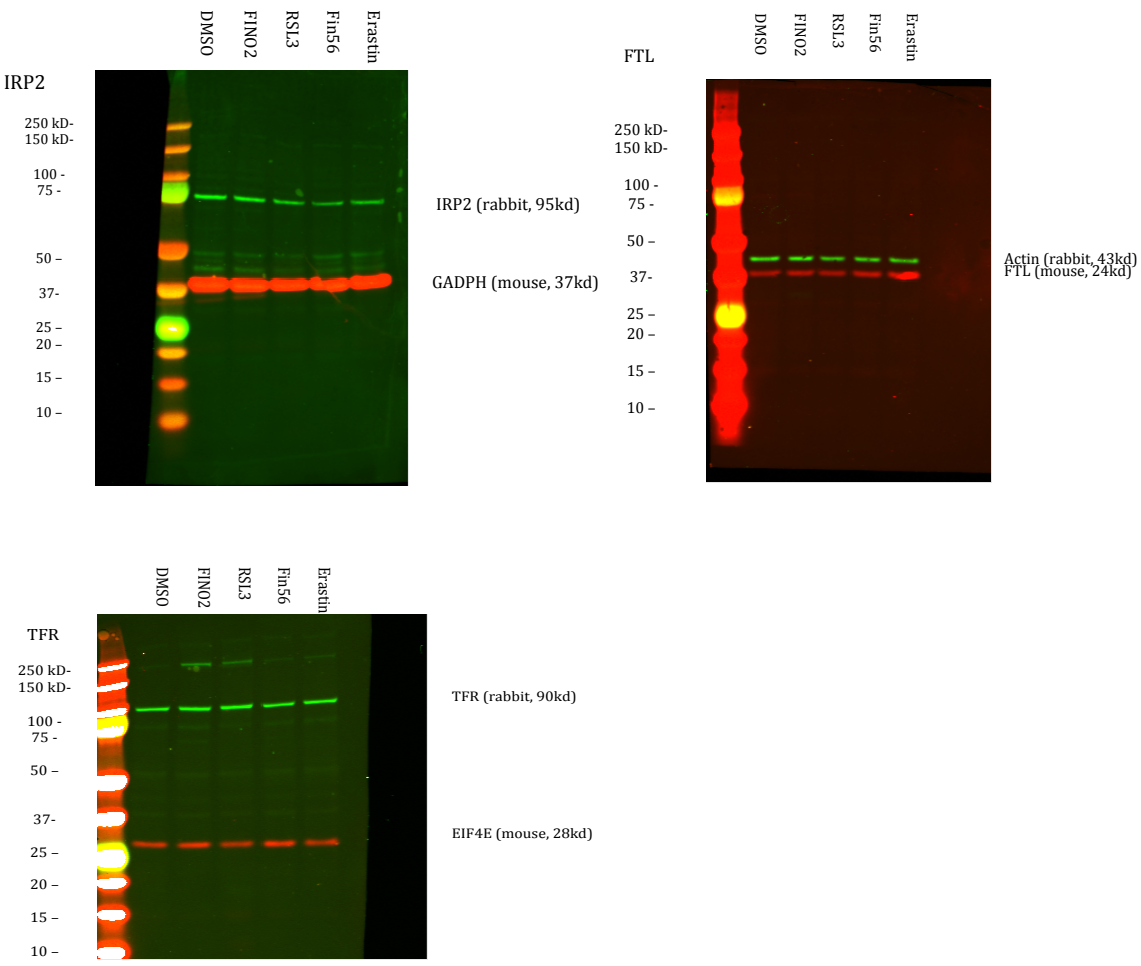

Supplementary Figure 13. Western blots of iron regulatory proteins in cells treated with vehicle (DMSO) or ferroptosis inducers. Experiments were performed in biological triplicate.

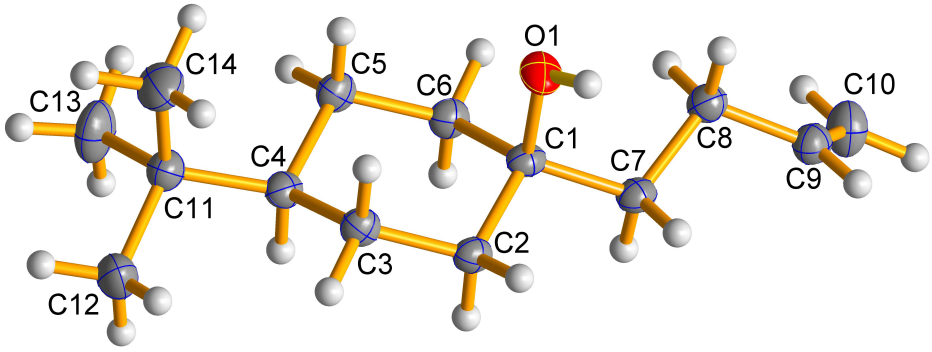

Supplementary figure 14. Crystal structure of **17a**

Supplementary table 1 Retention times and m/z for LC-MS analysis of in vitro Pharmacokinetic studies.

Compound	**Retention time**	**m/z**
Terfenadine	3.1 min	472.3
Ferrostatin-1	3.3 min	263.1
$FINO_2$	3.6 min	279.2
Lovastatin	3.7 min	405.2